Environ. Sci. Technol. **1999**, *33,* 874−881

Photodecomposition of the Carbamate Pesticide Carbofuran: Kinetics and the Influence of Dissolved Organic Matter

JOHN BACHMAN† AND
HOWARD H. PATTERSON*
Department of Chemistry, University of Maine, Orono, Maine 04669

This study examined the photodecomposition of carbofuran, a carbamate pesticide with high oral toxicity. Rate constants are measured for the pesticide in aqueous solution and in the presence of various samples of dissolved organic matter (DOM). Kinetic experiments are monitored with HPLC, while reaction products are determined using HPLC, GC−MS, and ^{1}H NMR: mechanisms are proposed for the first three steps of the reaction. It was found that the photodecomposition proceeds via first-order reaction kinetics and that the presence of various DOM samples inhibits the photolysis reaction of carbofuran. This phenomenon can be correlated to the magnitude of the binding interaction between carbofuran and DOM. Finally, techniques such as GC−MS and ^{1}H NMR are used to identify the photodecomposition products. The first three steps of the reaction are defined. In the first step of the reaction, the carbamate group is cleaved from the molecule. The furan moiety is opened in the second step producing a substituted catechol with a *tert*-butyl alcohol group as the substituent at the number three carbon. This molecule then undergoes a dehydration reaction to form an alkene side group from the *tert*-butyl alcohol side group.

Introduction

The use of pesticides is an integral part of world food production as illustrated by the fact that more than 2.5 million tons of these anthropogenic chemicals were applied to soil and foliage in 1996 (*1*). Recent findings that cite the presence of pesticides in drinking water supplies illustrate the fact that some fraction of pesticides applied to a particular location can be transported off site and into surface waters (*2*). Specifically, the carbamate pesticide carbofuran has been found in surface water that serves as a drinking water source for Sacramento, CA (*3*). Given the potential human and wildlife health risks associated with toxic pesticides in surface waters (*3, 4*), it is important to determine the probability that a certain chemical will persist in the environment by examining the various reactions of the molecule. Transformations such as microbial, chemical, and photochemical degradation are recognized as the significant processes in determining the fate and transport of pesticides.

* Corresponding author phone: (207)581-1178; fax: (207)581-1191; e-mail: howardp@maine.maine.edu.
† Present address: Great Lakes Environmental Center, 739 Hastings St., Traverse City, MI 49686.

Photochemical reactions are especially important in the realm of wastewater treatment as a technique used to remove harmful chemicals from the waste stream. (*5*). To effectively employ photolysis as a water treatment technique, the reaction of the chemical of interest must be thoroughly studied including the subsequent reactions of intermediates. Ollis et al. (*5*) point out that, since complete removal of harmful chemicals is the goal in wastewater treatment, demonstration of the formation and elimination of intermediates is required to show that complete remediation has been achieved. Hence, both kinetic and mechanistic data are needed to fully understand the photochemical reaction.

Dissolved organic matter (DOM), ubiquitously present in soils and surface waters, also plays an important role in regard to pesticide decomposition. Binding interactions to DOM have been shown to slow the rate of microbial degradation of pesticides (*6*). DOM is the primary light-absorbing species in surface water and, as a result, plays an important role in photochemical reactions taking place in surface water. Additionally, reports have found DOM can either enhance (*7*) or inhibit the rate of photolysis (*8*). Photochemical decomposition of pesticides represents an important transformation pathway that can occur in surface waters and in soil.

Carbofuran is a broad spectrum insecticide with a high oral toxicity. The oral LD50 for carbofuran is 11 mg/kg body weight in rats (*9*). As a comparison, the LD50 for parathion (an extremely toxic organophosphorus pesticide) is 8 mg/kg whereas the LD50 for atrazine (a triazine herbicide of low to moderate toxicity) is 1300 mg/kg (*10*). Carbofuran is used in the cultivation of corn, rice, cotton, and other crops. and its mode of action is cholinesterase inhibition (*11*). A comparative examination of the kinetics of the photolysis of the three carbamate pesticides aldicarb, carbaryl, and carbofuran has been published (*12*), and the relative rates (from fastest to slowest) can be listed as aldicarb, carbaryl, and carbofuran. However, individual rate constants have not been determined for the various pesticides. Some work has been performed on the photochemical degradation of carbofuran. Chiron et al. have recently published a report on carbofuran degradation by natural sunlight and a xenon arc lamp (*13*). Two decomposition products were identified by LC−MS, 3-hydroxy-7-carbofuranphenol as a product of hydrolysis and 2-hydroxy-3-(2-methylprop-1-enyl)-phenyl-*N*-methylcarbamate as a rearrangement product. Raha and Das (*14*) examined the photodecomposition of 1000 ppm solutions of carbofuran in various solvents. They reported two products for aqueous solutions of carbofuran that had been irradiated by natural sunlight for 5 days, 2,3-dihydro-2,2-dimethylbenzofuran-4,7-diol and 2,3-dihydro-2,2-dimethyl benzofuran-7-yl *N*-methylcarbamate.

This paper examines both kinetic and mechanistic aspects of the photochemical degradation of carbofuran. In addition, we examine the role of humic materials (DOM) in regulating this photolysis reaction using DOM from several different sources. The goals of this research are (i) to determine the photodecomposition kinetics of carbofuran, (ii) to determine the effect of dissolved organic matter on reaction rate, and (iii) to determine the photodecomposition reaction products.

Experimental Section

Materials. Carbofuran (2,3-dihydro-2,2-dimethylbenzofuran-7-ol *N*-methylcarbamate) and 2,3-dihydro-2,2-dimethylbenzofuran-7-ol were purchased from ChemService and were used as received (99% purity). Phosphomolybdic acid solution was used to visualize TLC experiments. A 20% (w/v) solution

10.1021/es9802652 CCC: $18.00
Published on Web 01/30/1999

of phosphomolybdic acid was purchased from Aldrich Chemical Co. It was further diluted to 10% (w/v), and 5% (v/v) concentrated sulfuric acid was added prior to use. The solvents dichloromethane, ethyl acetate, and hexane were purchased from EM Science. HPLC-grade methanol and acetonitrile from EM Science were used for HPLC experiments. All ^{1}H NMR experiments were conducted in deuterated chloroform purchased from Aldrich Chemical Co. The $CDCl_3$ was supplied with 0.03% tetramethylsilane as an internal reference. All solvents were used as received.

Collection and Preparation of DOM Samples. One soil sample and one water sample were collected for use in the photochemical experiments. The organic surface horizon was collected from a stand of red pine in Orono, ME (November 1995). Soil cores, approximately 8 cm deep and 5 cm in diameter, were collected from random sites within the stand of trees. The forest soil, litter, and humus was dark in color and included fallen pine needles. The subsamples were combined and stored at 4 °C prior to extraction and filtration.

An additional sample of organic matter was collected from Caribou Bog in Orono, ME. This wetland site is described as a sphagnum bog. To collect water from the bog, the vegetation was pushed aside and the void was allowed to fill with water. Cleaned and sterilized 1-L nalgene bottles were submerged in the water and allowed to fill. The water was dark in color and turbid. A total of 2 L was collected and stored at 4 °C prior to filtration.

A humic acid and a fulvic acid sample used in the photochemical experiments were purchased from Aldrich Chemical Co. and provided by Dr. Christopher Cronan from the Program in Ecology and Environmental Science, University of Maine, respectively. The Aldrich humic acid sample was determined to be 40.7% C. The fulvic acid sample was isolated from a southern hardwood forest soil, and carbon content of this sample was 47.2% C. Both the humic and fulvic acids were received as brown solid material that was stored in a desiccator prior to use in the photolysis experiments.

To separate the organic matter from the pine forest soil sample, approximately 1.5 kg of soil was placed in a 2-L nalgene bottle and 1500 mL of distilled, deionized water was added. The sample was extracted for 24 h at room temperature with periodic shaking. Following the extraction, the liquid from the pine forest soil extract was darkly colored and turbid.

The remaining steps of sample processing apply to both the pine forest soil sample and the water sample collected from the bog. The soil extract and the water sample were passed through a series of filters to remove clay particles, plant debris, and other unwanted particulates. First, the samples were passed without vacuum through Whatman 41 ashless filter paper. The resulting filtrant was passed through a Gelman A/E glass fiber filter with a pore size of 1 μm with the aid of vacuum. The final filtration was conducted with a Gelman A/E glass fiber filter with a pore size of 0.45 μm, again, using vacuum filtration. At this point the samples were no longer turbid. The bog sample and the coniferous sample were both deep amber in color.

Following filtration, the samples were passed through a cation exchange column. Columns with inside diameters of 4.5 mm were packed with Rexyn 101H beads. The packing material had previously been Soxhlet extracted with methanol to remove residual carbon. The pumping sequence through the column was as follows: 1 M HCl for 15 min to condition the packing material, distilled/deionized (dd) H_2O for 30 min, DOM sample. Approximately 200 mL of DOM sample was collected at a time. Following sample collection, the columns were flushed with water (10−15 min) and the HCl/H_2O conditioning step was repeated. Finally, the samples were quantified in terms of carbon content with a calibrated total organic carbon analyzer (O.I. Corp. model 700).

Photochemical Reaction Cell. All irradiations were performed with an EF-260C UV lamp from Spectronics Corporation (Westbury, NY). The lamp emits a narrow band of radiation at 254 nm. The irradiation experiments did not employ additional filters or monochromators. The light source contains two 6-W tubes that are 8 cm long. Typical output is 810 $\mu W/cm^2$. Samples were irradiated in quartz tubes (1 mm thick). Tube dimensions were 12.5 mm i.d. and 100 mm length. A maximum of seven tubes could be irradiated at the same time. The distance from the light source to the middle of the sample tube was 3.8 cm. Irradiation samples reached a maximum temperature of 28 °C in approximately 30 min. Solutions were not agitated or mixed during exposure.

The photochemical reaction cell was characterized using a potassium ferrioxylate actinometer as described in *Photochemistry* by Calvert and Pitts (*15*). The calculated value of the extinction coefficient was 1.18×10^4 L mol^{-1} cm^{-1}, which is in good agreement with the published value of 1.10×10^4 L mol^{-1} cm^{-1}. Lamp flux was determined by irradiating the potassium ferrioxylate reactant for 12 s and determining the number of Fe^{2+} molecules produced. The average value of the flux is 2.664×10^{16} photons/s, with a range of 2.77×10^{16} to 2.58×10^{16} photons/s.

All solutions for the photolysis experiments were prepared immediately prior to irradiation. Solutions were made in an appropriately sized volumetric flask and then immediately transferred to a nalgene bottle. Long periods of storage in glass were avoided to prevent loss of carbofuran due to molecules adhering to the glass walls of the flask. Exactly 4 mL of the solution to be irradiated was pipetted into the reaction tubes. Typically, six reaction tubes were irradiated simultaneously. At various times, two reaction tubes were collected for each data point. The contents of the two tubes were stored in a small (20 mL) nalgene bottle until HPLC testing could be started. Again, the solution was stored in nalgene to avoid loss of carbofuran due to adhesion to glass. Quantification by HPLC was performed as soon as possible following the completion of the irradiation experiment.

Product Separation. To identify the decomposition products, a suitable quantity of each compound had to be generated and isolated. To maintain consistency to the kinetics experiments, a series of irradiations were conducted with 30 ppm aqueous solutions of carbofuran. Following irradiation, the aqueous solution was saturated with sodium chloride to improve extraction efficiency. The reaction products were extracted with five 15-mL portions of ethyl acetate. Ethyl acetate was removed by rotary evaporation until the sample volume was approximately 1 mL.

The product mixture was analyzed with HPLC and GC−MS. Both techniques indicated that the mixture contained seven compounds. These products were separated via preparative thin-layer chromatography (TLC) using plates purchased from VWR Scientific (Merck, Item 13894). The stationary phase was 0.50 mm layer of 60 mesh silica, containing no fluorescent indicator, and coated onto a 20 × 20 cm glass plate. The mobile phase consisted of 3:1 hexane: ethyl acetate. As many as three developments of the TLC plate were required to achieve adequate separation. Products were visualized with an alcoholic phosphomolybdic acid solution. The indicator was applied to both vertical edges of the TLC plate and dried with a heat gun.

Upon visualization, the silica from the appropriate region of the plate was removed with a razor blade. The compound was resolvated by placing the silica in 100 mL of ethyl acetate and stirring for 10 min. The silica was removed with vacuum filtration. Again, the excess solvent was removed via rotary evaporation.

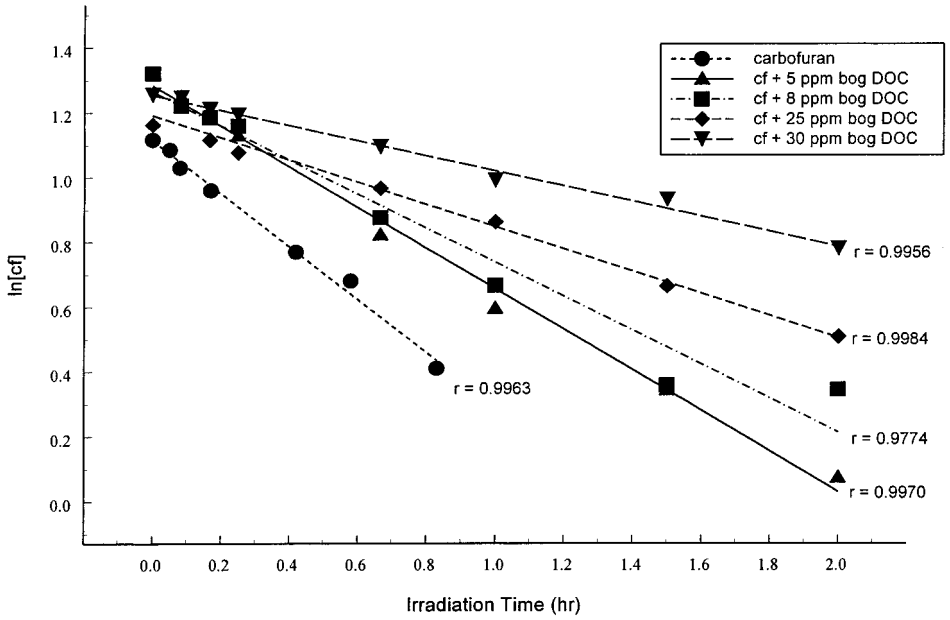

FIGURE 1. Rate plots for the irradiation of carbofuran in the presence of various concentrations of DOM.

Instrumentation. The technique of synchronous scan fluorescence spectroscopy (SSFS) involves scanning both the excitation and emission monochromators over a specified range of wavelengths. In typical emission fluorescence spectroscopy, the excitation monochromator is fixed at a particular wavelength while the emission monochromator is scanned. In SSFS, a constant wavelength difference ($\Delta\lambda$) is maintained between the excitation and emission monochromators as they scan the specified spectral range. SSFS measurements were collected on a model QM-1 fluorescence spectrometer from Photon Technologies International (PTI), Inc. The instrument is equipped with a 75-W xenon arc lamp. Excitation slit widths were typically set at 1 nm with the emission slits set at 10 nm. A $\Delta\lambda$ value of 27 nm was used for all SSFS measurements. Quartz fluorimetry cuvettes with a path length of 10 mm were used for all fluorescence and absorption spectroscopy measurements.

GC−MS measurements were made on a Hewlett-Packard 5890 gas chromatograph with Hewlett-Packard MSD 5970 serving as the detector. Two chromatography columns were used in the analyses, specifically a 30 m × 0.25 mm i.d. DB-5ms column from J&W Scientific and a 30 m × 0.25 mm 50% phenyl silicone column from Quadrex. Components of the various samples were separated using the following parameters: injector temperature set to 100 °C, the initial oven temperature of 100 °C was held for 3 min, the temperature was then ramped to 180 °C at a rate of 25 °C/min. The oven was held at 180 °C for 1 min and then ramped to a temperature of 250 °C at a rate of 10 °C/min and held at this temperature for 5 min. The detector temperature was set at 320 °C, and the injector was set at 100 °C. Helium was used as the carrier gas with a flow rate of 50 mL/min. Prior to injection, samples were filtered through a Gelman 2 mm Acrodisc syringe filter (0.2 μm pore size) to remove small particles that could obstruct flow through the column.

HPLC was used to quantify the samples from the photolysis experiments. Samples were analyzed on a Hewlett-Packard model 1050 high-performance liquid chromatograph. The detector was a UV/vis diode array detector, model 1040A. Separations were made on a Columbus C-18 column, 150 mm × 4.6 mm, 5μm particle size. Samples were injected by a Hewlett-Packard model 1050 autosampler. Injection size was either 20 or 95 μL depending on initial carbofuran concentration. Flow rate was 1 mL/min for all experiments. The mobile phase used for all experiments was 45.45% water, 45.45% methanol, and 9.10% acetonitrile. The detector was set to monitor 276 and 216 nm. Authentic samples of carbofuran and 2,3-dihydro-2,2-dimethylbenzofuran-7-ol were analyzed to determine separation parameters and retention times. Calibration standards of the two compounds were prepared for both injection volumes. Calibration curves were linear and had excellent correlation coefficients (carbofuran, 20 μL injection, $r = 0.9999$; carbofuran, 95 μL injection, $r = 0.9983$; 2,3-dihydro-2,2-dimethylbenzofuran-7-ol, 20 μL injection, $r = 0.9987$; and 2,3-dihydro-2,2-dimethylbenzofuran-7-ol, 95 μL injection, $r = 0.9894$).

Proton NMR spectra were collected on a 300 MHz Varian Gemini XL 300. Peaks were referenced to an internal TMS standard. Sample concentrations were approximately 5 mg/mL.

Results and Discussion

Kinetic Experiments. Carbofuran was irradiated in aqueous solution and in the presence of DOM; samples for quantitation of carbofuran were collected over a period of approximately 2 h. The concentration of the pesticide was determined by HPLC using a comparison of peak area to a standard curve. The data were plotted as the natural log of carbofuran concentration (ln[cf]) versus irradiation time. All experiments produced linear plots of ln[cf] vs *t*, indicating that the photochemical degradation reaction is first order in carbofuran. The first-order rate constants for 3 and 0.5 ppm carbofuran solutions are 0.76 and 0.69 h^{-1}, respectively.

Experiments were conducted with 3 ppm initial carbofuran concentration and various concentrations of the four DOM samples. Again, all experiments produced linear first-order rate plots, allowing for the calculation of the rate constants. In all cases the presence of DOM slowed the rate of photolysis. For example, experiments conducted with 3 ppm carbofuran and various concentrations of the bog DOM sample produced the following rate constants: 0.62, 0.51, 0.45, 0.32, and 0.23 h^{-1} for solutions with 5, 8, 15, 25, and 30 ppm DOM, respectively. Figure 1 displays the rate data from these experiments. One can see that increasing the DOM concentration decreases the slope of the rate plots, indicating a decreasing reaction rate. The data from all the experiments with other DOM samples are summarized in Tables 1−3.

TABLE 1. Rate Constants, 3 ppm Carbofuran with Various DOM Concentrations

	DOM concn				
DOM sample	5 ppm	8 ppm	15 ppm	25 ppm	30 ppm
bog	0.62 h^{-1}	0.51 h^{-1}	0.45 h^{-1}	0.32 h^{-1}	0.23 h^{-1}
pine	0.58 h^{-1}	0.51 h^{-1}	0.40 h^{-1}	0.25 h^{-1}	0.24 h^{-1}

TABLE 2. Rate Constants, 3 ppm Carbofuran with Various Concentrations of Aldrich Humic Acid (aha)

	DOM concn		
DOM sample	3.4 ppm	10.2 ppm	20.4 ppm
aha	0.47 h^{-1}	0.27 h^{-1}	0.16 h^{-1}

The rate constant data clearly show that the presence of DOM slows the rate of carbofuran photolysis. The magnitude of rate inhibition is different for each of the four DOM samples. For a given DOM concentration, the bog DOM sample produces the least amount of rate reduction followed by the pine sample, the southern hardwood fulvic acid, and, finally, the Aldrich humic acid sample. The rate effects are not linearly related to DOM concentration.

It was postulated that the decrease in the rate of photodegradation could be due either to DOM competing with carbofuran for the available photons or to binding between DOM and carbofuran. Competing photochemical reactions were initially investigated as the cause of the measured rate effect. It is clear from the spectroscopic data that the DOM does react in the presence of light (Figure 2). Additionally, it has been reported elsewhere that DOM can react photochemically (*16*). However, the amount of light needed for the carbofuran reaction is small relative to the total flux from the lamp. For example, at the highest DOM concentration used (30 ppm), it can be determined through photometry experiments that DOM is absorbing 58.3% of the total flux while a 3 ppm solution of carbofuran absorbs 18.7% of the total flux. Thus, in the presence of DOM there remains a sufficient amount of photons in the system for the carbofuran photolysis. Given the magnitude of the lamp flux and the concentrations of the experimental solutions, it is not possible to account for the total of rate decrease with a competing photochemical pathways model. One of the shortcomings of this model is that it can only account for the absorption due to carbofuran and DOM but ignores the third species present, the bound form of carbofuran.

Alternatively, a second model to describe our photochemical results has been considered in which binding interactions partition a significant quantity of the pesticide molecules into a bound form. When carbofuran and DOM are in solution together, a certain fraction of the pesticide is bound to the DOM. It is believed that binding occurs predominantly through a hydrophobic partitioning mechanism, with polar interactions playing a much smaller role (*17, 18*). Representing the bound carbofuran as cf-DOM, the following equilibrium can be written:

$$\text{cf} + \text{DOM} \leftrightarrow \text{cf-DOM} \quad (1)$$

$$k_b = [\text{cf-DOM}]/[\text{cf}][\text{DOM}] \quad (2)$$

The binding constant, k_b, can be determined by a fluorescence quenching method. Carbofuran lends itself to this method since it has a strong fluorescence peak especially when measured by SSFS. It was determined experimentally that carbofuran has a maximum fluorescence intensity when spectra are collected with a $\Delta\lambda$ of 27 nm; thus, this parameter

TABLE 3. Rate Constants, 3 ppm Carbofuran with Various Concentrations of Southern Hardwood Fulvic Acid (shfa)

	DOM concn		
DOM sample	5 ppm	7.2 ppm	15 ppm
shfa	0.48 h^{-1}	0.42 h^{-1}	0.26 h^{-1}

was used in the fluorescence quenching experiments. As the amount of free carbofuran in solution is decreased due to binding to DOM, the fluorescence intensity is also decreased. The magnitude of fluorescence intensity reduction is determined by the DOM concentration and the binding constant. The Stern−Volmer equation defines the fluorescence quenching/binding relationship:

$$F/F_0 = 1 + k_b[\text{DOM}] \quad (3)$$

where F is the fluorescence intensity of carbofuran/DOM solution, F_0 is the fluorescence intensity of carbofuran, k_b is the binding constant, and [DOM] is the DOM concentration.

Fluorescence data were collected on carbofuran solutions with various DOM concentrations such that binding constants could be determined. Specifically, the Caribou Bog DOM sample had a binding constant (k_b) of 1.75×10^4 L/kg. The binding constants for the red pine, southern hardwood fulvic acid, and Aldrich humic acid were 2.2×10^4, 4.10×10^4, and 4.26×10^4 L/kg, respectively. It can be noted that the ranking of DOM samples from least to most, in terms of rate effects (bog, pine, southern hardwood fulvic acid, Aldrich humic acid), is the same as the ranking of binding constants (bog, pine, southern hardwood fulvic acid, Aldrich humic acid).

To further illustrate that the photolysis rate effects are a result of binding interactions, one can examine the rate constant data as related to the percent of bound carbofuran in solution. The percentage of bound pesticide is calculated using the binding constant and the DOM concentration:

$$\%\ \text{bound} = (k_b[\text{DOM}])/(1 + k_b[\text{DOM}]) \times 100 \quad (4)$$

For example, at a concentration of 15 ppm, the bog DOM sample binds 21.3% of the total carbofuran concentration, while the Aldrich humic acid (15 ppm) binds 39.0% of the total carbofuran in solution. The rate constants for the same two DOM samples at 15 ppm are 0.45 and 0.27 h^{-1} for the bog and Aldrich humic acid, respectively. It can be noted that an approximately 2-fold increase in the amount of carbofuran bound in solution (20.3% vs 39.0%) is reflected in an approximately 2-fold decrease in the rate constant (0.45 and 0.27 h^{-1}).

To test if all of the experimental data fit this model, a plot of rate constant versus percent of carbofuran bound to DOM was prepared (Figure 3). When the data are plotted in this fashion, the four DOM samples produce essentially equivalent straight lines. Therefore, the photolysis rate constant is inversely proportional to the amount of bound pesticide. Although four different DOM samples were used in these experiments, the amount of rate reduction can be related (inversely) to the binding ability of the DOM, regardless of which particular DOM sample is considered. Also, the data in Figure 3 indicate that a single mechanism is responsible for the binding in all four DOM samples. As mentioned previously, it is believed that the binding mechanism is hydrophobic partitioning. Therefore, we conclude that all of the experimental data can be described by a model in which the magnitude of the DOM−pesticide binding is inversely proportional to the photolysis rate reduction.

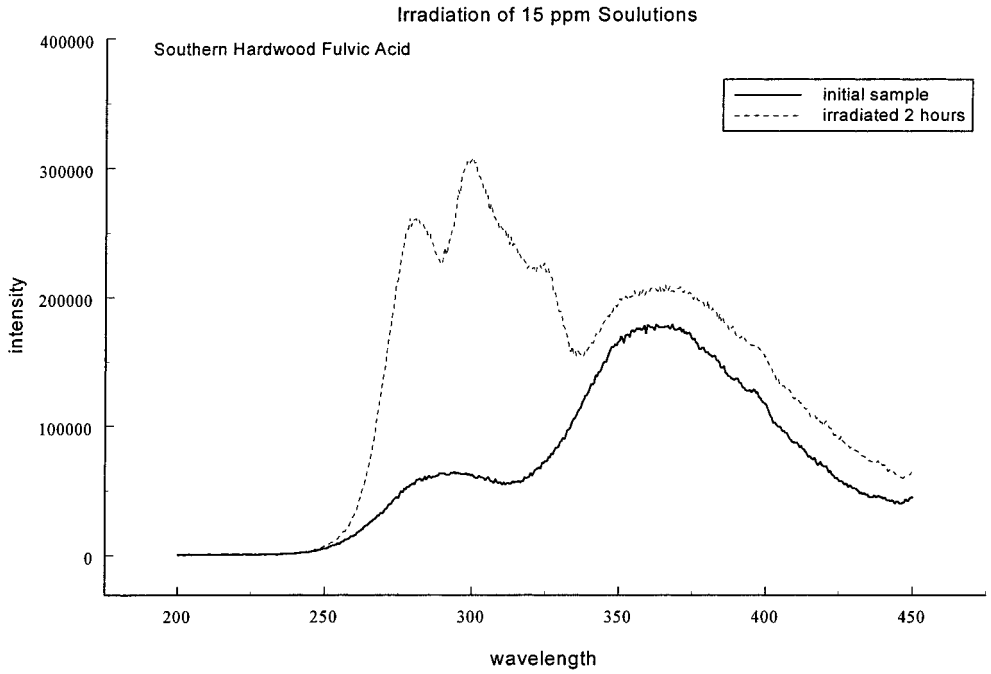

FIGURE 2. Synchronous scan fluorescence spectra ($\Delta\lambda = 27$ nm, optical path length = 10 mm) of southern hardwood forest DOM, initial and irradiated for 2 h.

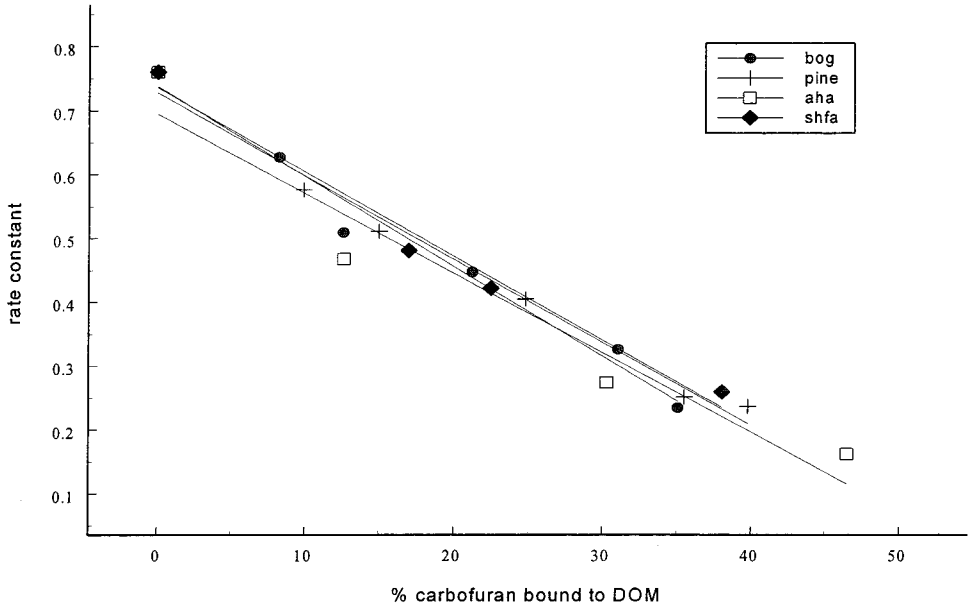

FIGURE 3. Rate constants for the photolysis of carbofuran/DOM solutions versus the percent of bound carbofuran in the corresponding solution.

It is clear that the magnitude of the DOM−carbofuran binding controls the magnitude of the photolysis rate effects. However, a physical picture is needed to fully understand the rate effects of DOM. The hydrophobic binding mechanism draws the carbofuran into an aggregate of humic molecules. This arrangement allows carbofuran to transfer the excess energy resulting from the absorption of a photon to the surrounding DOM molecules. Examination of the absorption spectrum of a mixture of carbofuran and DOM shows that carbofuran is still able to absorb photons despite being bound to DOM. Absorption spectroscopy (Figure 4) shows that the absorbance at 276 nm of a 3 ppm carbofuran solution is 0.392, a 30 ppm bog DOM solution is 0.358, and a mixture of 3 ppm carbofuran and 30 ppm bog DOM is 0.760 or roughly the sum of the two individual absorbances. However, fluorescence quenching and reduced photochemical reaction rates indicate that the energy absorbed by the carbofuran in the mixture is released via an alternative process such as energy transfer to DOM.

Identification of Intermediates and Products. The first step of the photochemical reaction of carbofuran in water is similar to its base hydrolysis reaction. Namely, the carbamate group is cleaved from the molecule to form 2,3-dihydro-2,2-dimethylbenzofuran-7-ol and carbamic acid. This step was confirmed by multiple experimental techniques. Peaks in both the GC−MS and HPLC chromatograms matched the respective retention times for an authentic sample of 2,3-dihydro-2,2-dimethylbenzofuran-7-ol. The fact that the retention times from the two chomatographic techniques match the retention times for the standard compounds is strong evidence that the identity of the decomposition product is 2,3-dihydro-2,2-dimethylbenzo-

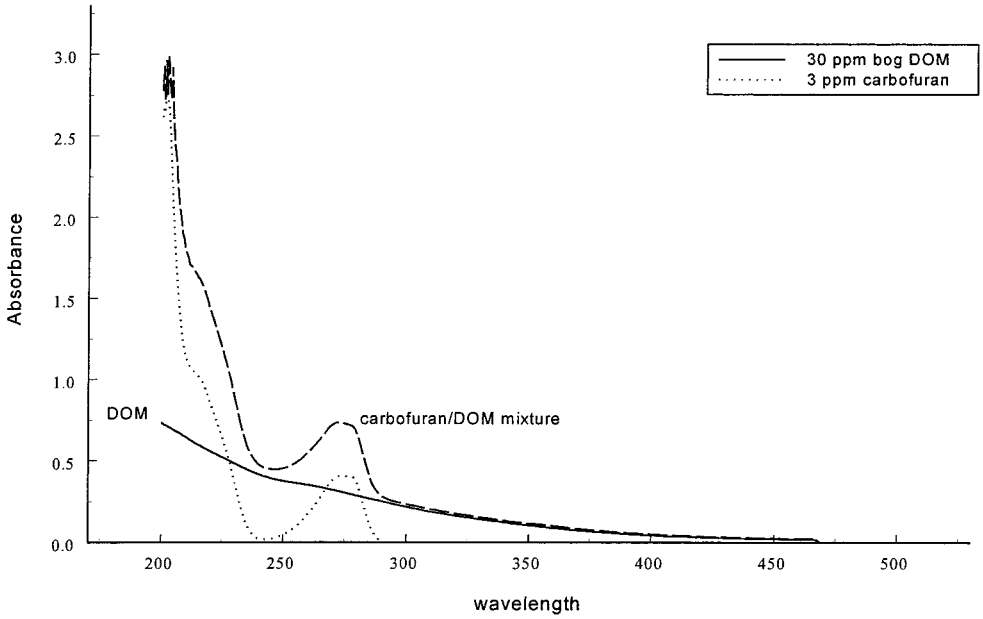

FIGURE 4. Absorption spectra of carbofuran, bog DOM, and carbofuran/DOM mixture (optical path length = 10 mm).

SCHEME 1. Photodegradation of carbofuran, steps 1 and 2.

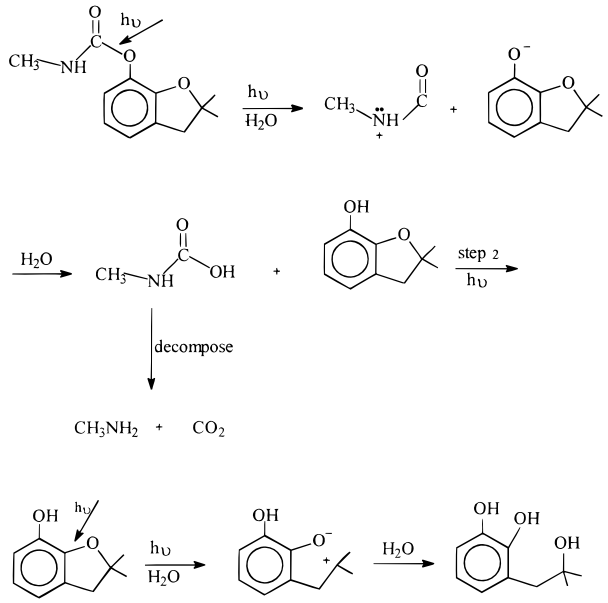

furan-7-ol. It is possible that a different molecule could elute at the same retention time. However, the mass spectra of the product found in the irradiated solution is identical to the mass spectra for the standard, confirming the identification.

The mechanism of the first three steps of the photodegradation of carbofuran is shown in Scheme 1. To produce 2,3-dihydro-2,2-dimethylbenzofuran-7-ol from carbofuran, the C−O bond of the carbamate group must be broken. The lamp used in the irradiation experiments produced a narrow line at 254 nm that corresponds to an energy of 470.9 kJ/mol. Carbon−oxygen single bonds require between 334.4 and 418.0 kJ/mol to cleave the bond; thus, sufficient energy is available in this system to break the bond. Cleavage of the C−O bond forms a phenolic anion and a cation on a basic nitrogen in the cleaved carbamate group (*19*). The phenolic anion can abstract a proton from the solvent (water) to form the intermediate, 2,3-dihydro-2,2-dimethylbenzofuran-7-ol. The cation can abstract an OH-, also from the water, to form carbamic acid, which is known to be unstable (*20*). Carbamic acid rapidly degrades to methylamine and carbon dioxide, both of which are gases at room temperature. The formation of the two gaseous products is a driving force for this reaction.

Analysis of the product mixture by GC−MS and HPLC shows a total of seven peaks including the parent molecule and 2,3-dihydro-2,2-dimethylbenzofuran-7-ol (Figure 5). Having analyzed the mixture with GC−MS, the molecular weights of the reaction products were obtained using GC−MS and are summarized in Table 4.

From these data, we identified the compounds at retention times of 10.5 and 6.6 min as carbofuran and 2,3-dihydro-2,2-dimethylbenzofuran-7-ol, respectively. These assignments are based on a comparison of retention times and mass spectra to standard molecules. The compounds appearing at the other retention times required further characterization before a confident identification could be made. The compounds were isolated using preparative TLC, and their structure was determined by comparing ^{1}H NMR analysis with the mass spectral data.

The ^{1}H NMR spectra for the compound at retention time 8.9 min (GC−MS) contains a multiplet at $\delta = 6.8$ ppm, a singlet at $\delta = 2.8$ ppm, and a singlet at $\delta = 1.3$ ppm. The integration of the peaks are approximately 3, 2, and 6, respectively. The multiplet at 6.8 ppm is assigned to three aromatic protons, the singlet at 2.8 ppm indicates two methylene protons, and the singlet at 1.3 ppm indicates six methyl protons.

The major ions in the mass spectra are as follows; m/z =182 (M^+), 167 (M − CH_3), 164, M − H_2O) and, 149 (M − $2CH_3$). Other significant ions are $m/z = 91$ corresponding to the benzyl ion and $m/z = 77$ corresponding to $C_6H_5^+$. From the available data, a chemical structure of the compound was determined as shown:

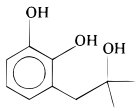

Having identified the reaction product, a reasonable mechanism must be outlined for the second step of the photolysis. As illustrated in the reaction scheme, the starting point of this reaction is 2,3-dihydro-2,2-dimethylbenzofuran-7-ol in which the C−O bond of the ether linkage in the furan moiety is broken. Opening of the furan group creates a negative charge that can be distributed over the aromatic

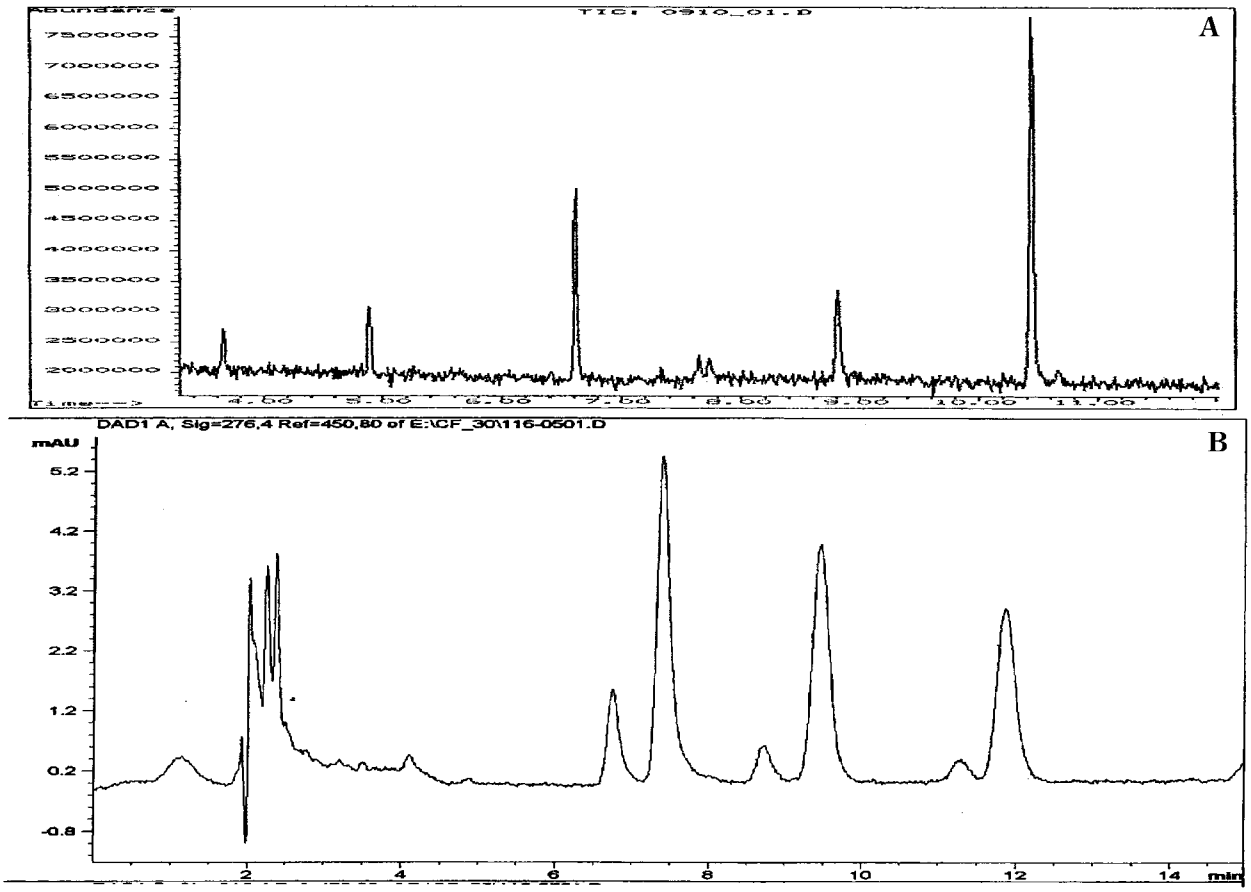

FIGURE 5. GC (A) and HPLC (B) chromatograms of the photolysis reaction mixture following 1 h of irradiation.

TABLE 4. GC−MS Data for Reaction Mixture

retention time	mol wt	mass of predominant ions in fragmentation pattern
10.5	221	221, 164, 149, 131, 91, 77
8.9	182	182, 167, 164, 149, 91, 77
7.7	164	164, 149, 131, 91, 77
7.4	166	148, 133, 108, 91, 77
6.6	164	164, 149, 131, 91, 77
4.9	148	148, 133, 105, 91, 77
3.7	126	126, 97, 55

ring and a positive charge that can be placed on the carbon at position 2 to form a tertiary carbocation. A water molecule can then add to the carbocation, with a charged species remaining at that position. The negative charge can then be released from the ring and deprotonate the H_2O to form a tertiary alcohol.

The product appearing at $r_t = 7.7$ min in the GC−MS chromatogram was also isolated and identified. The major ions in the mass spectra include $m/z = 164$ (M^+), 149 ($M - CH_3$), 131 ($149 - H_2O$), 91 ($C_6H_5CH_2^+$), and 77 ($C_6H_5^+$). This sample was derivatized with bis-trimethylsilyl acetamide (in excess), which converts a free alcohol to a trimethylsilyl (TMS) group. Two compounds are produced in the derivatization. The molecular weights of the derivatives are 236 and 308, as determined by GC−MS analysis. The addition of one TMS group adds 72 mass units to the molecular weight. Since $164 + 72 = 236$ and $164 + (2 \times 72) = 308$, the two derivatives formed correspond to the addition of one and two TMS units, respectively.

The NMR spectrum of the compound that elutes at 7.7 min was not well resolved since the amount of product collected was quite small. However, aromatic protons can be deciphered at $\delta = 6.6-6.9$ ppm. Also, three singlets appear at the following δ values: 1.25, 1.75, and 3.35 ppm. Also, there is a peak at 5.35 ppm, indicative of alkene protons. Due to the low resolution, the spectrum was not integrated. Using the available chromatographic and spectral data the following structure is assigned to the product of the third step of the photolysis of carbofuran. This compound results from the dehydration of the product of step two of the photolysis:

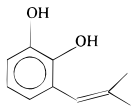

Chromatographic data indicate the presence of three additional products; however, the evidence is insufficient to propose structures for the remaining compounds. The mechanism results can be summarized as follows. Carbofuran decomposes via direct photolysis. In the first step of the reaction, the carbamate group is cleaved forming carbamic acid and 2,3-dihydro-2,2-dimethylbenzofuran-7-ol. Carbamic acid readily decomposes to carbon dioxide and methylamine. The phenolic product formed in the first step is also photochemically reactive. This molecule decomposes upon irradiation into a substituted catechol. The ether linkage of the furan group is cleaved forming a tertiary alcohol side chain attached to catechol. This molecule also reacts photochemically, converting the alcoholic side chain to an alkene via a dehydration reaction.

The present work demonstrates that the pesticide carbofuran degrades photochemically via a first-order reaction initially to 2,3-dihydro-2,2-dimethylbenzofuran-7-ol, which subsequently reacts to form additional products. Two of these

additional products have been identified. Also shown in this work is the fact that the presence of DOM slows the rate of photolysis of carbofuran. The magnitude of rate inhibition is directly proportional to the binding capacity of a particular DOM sample. Biological decomposition is also inhibited in the presence of DOM (*4*). Thus, DOM slows two important transformation pathways of carbofuran, thereby increasing its persistence.

Literature Cited

(1) Brown, L. R.; Flavin, C.; Kane, H. *Vital Signs-The Trends That Are Shaping Our Future.*;W. W. Norton: New York, 1996.
(2) Koplin, D. W.; Thurman, E. M.; Goolsby, D. A. *Environ. Sci. Technol.* **1996**, *30*, 335−340.
(3) Johnson, W. G.; Lavy, T. L. *J. Environ. Qual.* **1995**, *24*, 487−493.
(4) Nicosia, S.; Carr, N.; Gonzales, D. A.; Orr, M. K. *J. Environ. Qual.* **1991**, *20*, 532−539.
(5) Ollis, D. F.; Pelizzetti, E.; Serpone, N. *Environ. Sci. Technol.* **1991**, *25*, 1523−1529.
(6) Getzin, L. W. *Environ. Entomol.* **1973**, *2*, 461−467.
(7) Canonica, S.; Jans, U.; Stemmler, K.; Hoigne, J. *Environ. Sci. Technol.* **1995**, *29*, 1822−1831.
(8) Torrents, A.; Anderson, B. G.; Bilboulian, S.; Johnson, W. E.; Hapeman, C. J. *Environ. Sci. Technol.* **1997**, *31*, 1476−1482.
(9) Kuhr, R. J.; Dorough H. W. *Carbamate Insecticides: Chemistry, Biochemistry, and Toxicology*; CRC Press: Cleveland, 1976; p 8.
(10) Hayes, W. J., Jr., Laws, E. R., Jr., Eds. *Handbook of Pesticide Toxicology*; Academic Press: New York, 1991; p 1042.
(11) Briggs, S. A. *Basic Guide to Pesticides; Their Characteristics and Hazards*; Hemisphere Publishing: Washington, DC, 1994; p 201.
(12) de Bertrand, N.; Barcelo, D. *Anal. Chim. Acta* **1991**, *254*, 235−244.
(13) Chiron, S.; Torres, J. A.; Fernandez-Alba, A.; Alpendurada, M. F.; Barcelo, D. *Int. J. Anal. Chem.* **1996**, *65*, 37−52.
(14) Raha, P.; Das, A. K. *Chemosphere* **1990**, *21*, 99−106.
(15) Calvert, J.; Pitts, D., Jr. *Photochemistry*; John Wiley and Sons: New York, 1986; pp 781−789.
(16) Bruccoleri, A.; Pant, B. C.; Sharma, D. K.; Langford, C. H. *Environ. Sci. Technol.* **1993**, *27*, 889−894.
(17) Schwarzenbach, R. P.; Gschwend, P. M.; Imboden, D. M. *Environmental Organic Chemistry*; John Wiley and Sons: New York, 1993: pp 255−341.
(18) Xing, B.; Pignatello, J. J.; Gigliotti, B. *Environ. Sci. Technol.* **1996**, *30*, 2432−2440.
(19) Morrison, R. T.; Boyd, R. N. *Organic Chemistry*, 5th ed.; Allyn and Bacon: Boston, 1987; pp 202−206, 1041.
(20) McMurray, J. *Organic Chemistry*, 3rd ed.; Brooks/Cole Publishing: Belmont, CA, 1992; p 1204.

Received for review March 16, 1998. Revised manuscript received November 24, 1998. Accepted December 24, 1998.

ES9802652